Electrochemical Behaviors of Cr(III) in Molten LiF-NaF-KF Eutectic

*Wei Wu[1,2], Shaoqiang Guo[2,3, *], Jinsuo Zhang[2,3,*]*

[1] School of Chemical Engineering and Technology, Xi'an Jiaotong University, Xi'an 710049, China
[2] Nuclear Engineering Program, Department of Mechanical and Aerospace Engineering, The Ohio State University, Columbus, OH 43210, United States
[3] Nuclear Engineering Program, Department of Mechanical Engineering, Virginia Polytechnic Institute and State University, Blacksburg, VA 24060, United States
[*]E-mail: guos1987@vt.edu, zjinsuo5@vt.edu

The electrochemical properties and kinetics of chromium(III) in molten LiF-NaF-KF (46.5-11.5-42 mol %, FLiNaK) eutectic at 700 °C were studied by using cyclic voltammetry (CV) and square wave voltammetry (SWV). CV and SWV results indicate two steps of electron exchange process, corresponding to the reduction of Cr(III) to Cr(II) and Cr(II) to Cr(0) and the oxidation of Cr(0) to Cr(II) and Cr(II) to Cr(III). The redox of Cr(III)/Cr(II) is reversible, while the redox of Cr(II)/Cr(0) is quasi-reversible in the range of the scan rate investigated in this study. The reduction processes of Cr(III) to Cr(II) and Cr(II) to Cr(0) are diffusion-controlled according to the linear relationship between i_{pc} and the square root of scan rate (below 400 mV/s). The diffusion coefficients of Cr(III) and Cr(II) were calculated to be $(9.56\pm0.57)\times10^{-7}$ $cm^2 \cdot s^{-1}$ and $(3.68\pm0.09)\times10^{-6}$ $cm^2 \cdot s^{-1}$ at 700 °C, respectively. Also, the apparent standard potentials of Cr(III)/Cr(II) and Cr(II)/Cr(0) were estimated to be -0.215 V (vs. Pt) and -0.152 V (vs. Pt).

1. INTRODUCTION

Fluoride-salt-cooled high-temperature reactor (FHR) is a new reactor concept which uses liquid salts as coolant [1, 2]. LiF-NaF-KF eutectic (46.5-11.5-42 mol %, commonly referred to as FLiNaK) has been a promising candidate for the second loop of an FHR. However, during manufacture and storage of the fluoride salt, some oxidizing impurities (mainly including H_2O and HF) can ingress into the salt, which may induce corrosion of the high-temperature structural metals and alloys through the dissolution of active alloying elements into the melt [3]. Chromium is widely considered as the most

active transition metal element and can be preferentially dissolved into the fluoride salts in the form of ions because chromium has a much negative free energy of fluoride formation.

The nature of molten FLiNaK salt is ionic, and the oxidation and reduction of active transition metal elements like chromium must be electrochemical [4, 5]. Therefore, for better understanding the electrochemical behavior of chromium species in FLiNaK, it is important to obtain the electrochemistry-related fundamental data of chromium and its cations in molten FLiNaK salt. Several relevant experimental studies have been carried out. Yoko and Bailey [6] studied the reduction mechanism of Cr(III) in FLiNaK by means of cyclic voltammetry and chronopotentiometry at different temperature conditions. Ludwig et al. [7] measured the data about the electrochemical reduction and oxidation of Cr, as well as the dissolved Cr concentration, in FLiNaK salt at 650 °C through cyclic voltammetry and anodic stripping voltammetry. Peng et al. [8] investigated the two valence states of Cr in FLiNaK at 600 °C using cyclic voltammetry and square wave voltammetry. However, there is no study on the electrochemical feature and related parameters of Cr under the typical coolant temperature in FHR (at the temperature of 700 °C) [2]. The present study focused on the electrochemical behavior of chromium in LiF-NaF-KF eutectic at 700 °C. The electrochemical thermodynamic property (apparent potentials of Cr(III)/Cr(II) and Cr(II)/Cr(0)) and the transport property (diffusion coefficients of Cr(III) and Cr(II)) at 700 °C were obtained experimentally.

2. EXPERIMENTAL METHODS

The LiF-NaF-KF (46.5-11.5-42 mol %) eutectic salt (454 °C melting point and 1570 °C boiling point) was prepared by mixing the highly-purified anhydrous lithium fluoride (LiF), sodium fluoride (NaF) and potassium fluoride (KF) (greater than 99.5%, Sigma-Aldrich), and was used as the electrolytic bath. A small quantity of anhydrous chromium trifluoride (CrF_3) (>99.0% purity, Sigma-Aldrich) was added to the prepared LiF-NaF-KF salt to provide Cr(III). Before each experiment, the salt mixture would be dehydrated by heating up to 300°C under argon atmosphere for at least 8 hours. The salt was then melted to the desired experimental temperature in a nickel crucible. The crucible was in a graphite crucible which placed in an auto electro-melt furnace (Kerr Series 1361) (see Fig. 1).

All the electrochemical tests were carried out in a glove box system manufactured by Inert Technology. The glove box system was filled with purified argon gas, and the H_2O and O_2 in glove box were controlled under 5 ppm (see Fig. 1). A three-electrode system was applied to the electrochemical measurement. The counter electrode (CE) was a tungsten rod (φ 4.0 mm) with a large surface area of 1.3 cm^2 because tungsten is inert in the range of the applied potential in this study. The reference electrode (RE) was a platinum wire (φ 0.6 mm) because platinum can serve as a quasi-reference electrode in the molten salt with a stable potential associated with $Pt/PtO_x/O^{2-}$ when the O^{2-} concentration of the bath is constant [9, 10]. In our experiments, the oxygen concentration in the electrolyte was invariable during all the tests, because the crucible was open to the argon atmosphere and the oxygen partial pressure was controlled to be constant in the glove box. The working electrode (WE) was a pure tungsten wire (φ 1.6 mm) for cyclic voltammetry and square wave voltammetry. The surface area of the working electrode was measured according to the length of the tungsten wire

exposed to the melt by pulling the wire out from the salt until a dramatic increase of potential difference between WE and RE was observed. All electrochemical tests were performed with a Gamry Interface 1000 Potentiostat/Galvanostat/ZRA controlled by a computer using Gamry Instruments Framework software 7.03.

3. RESULTS AND DISCUSSION

3.1. Cyclic voltammetry

Cyclic voltammetry (CV) was used to investigate the electrode reaction mechanism of CrF_3 in molten FLiNaK salt. For ensuring the stability of experimental condition and the consistency of experimental data, five repeated cycles of the cyclic voltammetry of CrF_3 were conducted at each scan rate. Fig. 2 illustrates the cyclic voltammograms of CrF_3 in molten FLiNaK salt at 700 °C at various scan rates. The voltammograms shows four separated peaks: two reduction peaks (1c and 2c) at -0.245 V (vs. Pt) and -0.474 V (vs. Pt), respectively (see Fig. 3), and two oxidation peaks (1a and 2a) at approximately -0.071 V (vs. Pt) and around -0.242 V (vs. Pt), respectively (see Fig. 3). Peak 1c and 1a are attributed to the reduction of Cr^{3+} and the corresponding oxidation of low-valent Cr species formed during the anodic potential sweep. Peak 2c corresponds to the reduction of low-valent Cr to metal Cr. Peak 2a indicates the re-oxidation of the deposited Cr metal on the tungsten electrode.
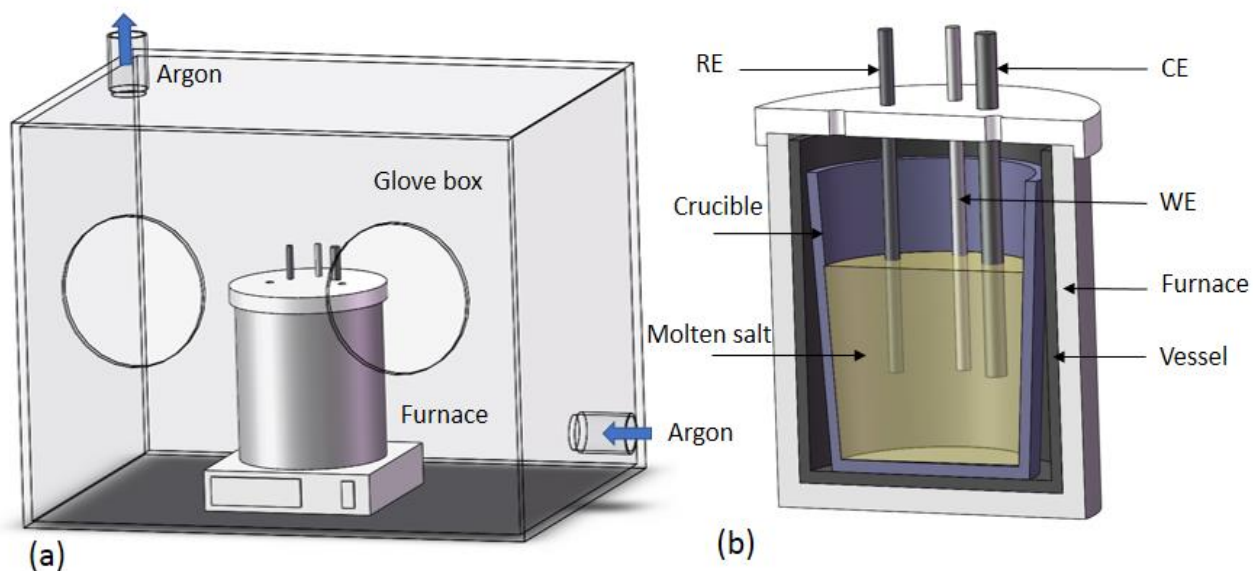

Figure 1. Schematic illustration of the experimental set-up (a) and the electrode system (b).
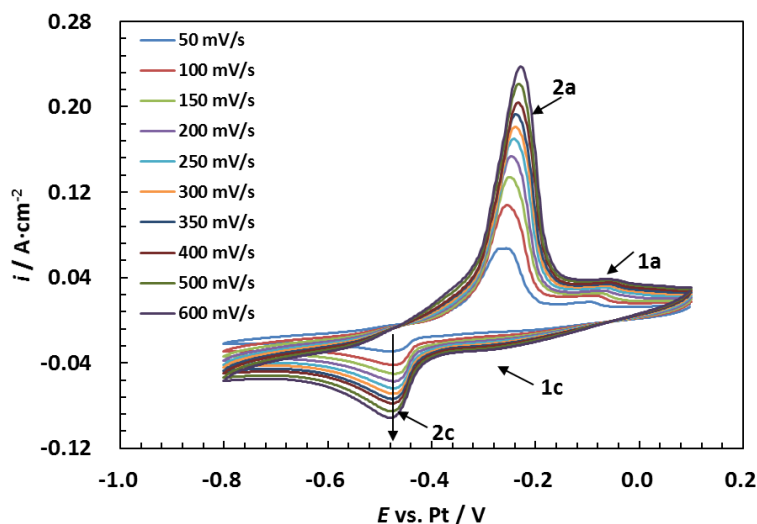
Figure 2. Cyclic voltammetry of 0.285 wt% CrF_3 in molten FLiNaK salt at 700 °C, working electrode: W (φ=1.6 mm, surface area: 0.64 cm^2), counter electrode: W (φ=4.0 mm), reference electrode: Pt wire.
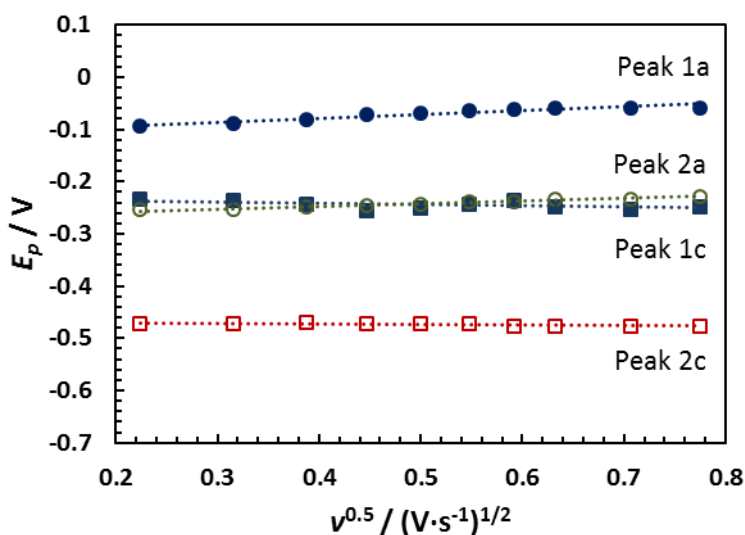

Figure 3. Plot of peak potential versus the square root of the potential scan rate of cyclic voltammetry in FLiNaK-CrF$_3$ (0.285 wt%) at 700 °C.

The ratio of the peak currents (i_{pa}/i_{pc}) of a CV curve is an inherent parameter for certain reaction system, and it is usually used to evaluate the reversibility of electrode reaction [11, 12]. The ratio of $|i_{p,1a}/i_{p,1c}|$ obtained is given in Table 1 which is around unity. This indicates that the redox of Cr(III)/low-valent Cr in this case is reversible and the electro-active species of the electrochemical reaction are both soluble in FLiNaK. As far as the redox of low-valent Cr/Cr(0), the ratio of $|i_{p,2a}/i_{p,2c}|$ from Table 1 was deviated from unity. Moreover, the anodic peak (Peak 2a) potential slightly shifted toward positive potentials with the potential scan rate increase, as shown in Fig. 1. These observations indicate that the redox of low-valent Cr/Cr(0) was quasi-reversible.

Table 1. Ratios of the anodic to cathodic peak current density.

v/V·s^{-1}	0.05	0.1	0.15	0.2	0.25	0.3	0.35	0.4	0.5	0.6
$|i_{p,1a}/i_{p,1c}|$	1.61	1.67	1.32	1.10	1.07	0.93	0.96	0.91	0.93	0.71
$|i_{p,2a}/i_{p,2c}|$	4.77	4.95	5.06	4.93	4.94	4.73	4.67	4.63	4.60	4.47

For a reversible reaction, the separation ($\Delta E_p = |E_{pc} - E_{pa}|$) between the reduction potential (E_{pc}) and the oxidation potential (E_{pa}) can be described by the equation [12]:

$$\Delta E_p = \frac{2.3RT}{nF} = \frac{0.193}{n} \; (973K) \tag{1}$$

where R the gas constant (8.314 J·mol^{-1}·K^{-1}), T the absolute temperature in K, F the Faraday's constant (96485 C·mol^{-1}), and n is the number of exchanged electrons. The value of ΔE_p for the FLiNaK-CrF$_3$ system was measured to be 0.234 V from Fig. 2. According to Eq. (1), the exchanged electron number of the reaction of Cr(III)/low-valent Cr was 0.824 (about 1). Therefore, the low-valent Cr is Cr(II), and the electrode reaction is attributed to two reduction steps: Cr(III) to Cr(II) and Cr(II) to Cr(0), and two corresponding oxidation steps: Cr(0) to Cr(II) and Cr(II) to Cr(III). These results are consistent with those reported by Yoko [6], Ludwig [7] and Peng [8].

Fig. 4 presents the plot of reduction peak current density versus the square root of the scan rate. The linear relationship for Peak 1c, as well as Peak 2c, is observed in the figure except at the high scan rates for Peak 1c (above 400 mV/s), which indicates that both the first and the second reduction steps of Cr(III) were controlled by ion diffusion [12] when the scan rate is below 400 mV/s. This linear relationship also proves the reversibility of the reduction mechanism of Cr(III).
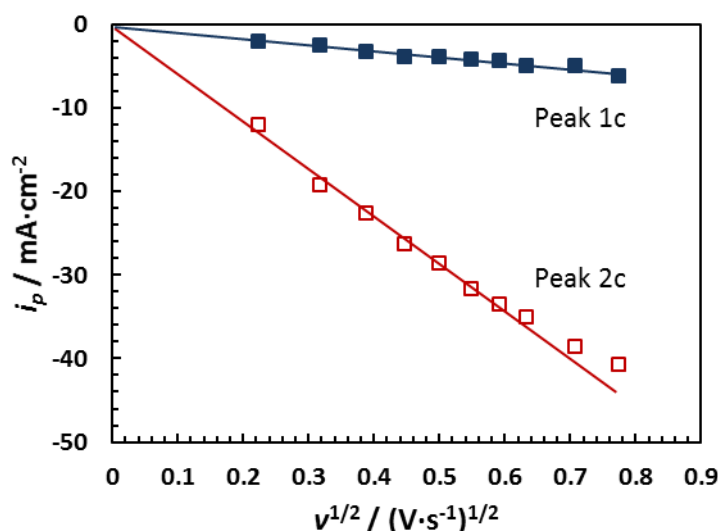

Figure 4. Relationship of CrF$_3$ reduction peak current density versus the square root of the potential scan rate of cyclic voltammetry in FLiNaK-CrF$_3$ (0.285 wt%) at 700 °C.

For a reversible soluble-soluble system, i.e., Cr(III)/Cr(II) in this case, the peak current is correlated to the potential scan rate by using Randles-Sevcik equation

$$I_{p,1c} = -0.4463nFSC_{Cr^{3+}} \left(\frac{nF}{RT}\right)^{0.5} D_{Cr^{3+}}^{0.5} v^{0.5} \tag{2}$$

where S the electrode surface area (cm^2), $C_{Cr^{3+}}$ the concentration of Cr^{3+} in the melt (mol·cm^{-2}), $D_{Cr^{3+}}$ the diffusion coefficient of Cr^{3+} (cm^2·s^{-1}), and v the potential scan rate (V·s^{-1}). The correlation $\rho_{FLiNaK}(kg/m^3) = 2579.3 - 0.624T$ [13] was used to convert mass percent of Cr^{3+} in FLiNaK-CrF$_3$ to molar concentration. Using Eq. (2), $D_{Cr^{3+}}$ in FLiNaK can be calculated to be $(9.56\pm0.57)\times10^{-7}$ cm^2·s^{-1} at 700 °C, which falls in between 5.9×10^{-7} cm^2·s^{-1} at 716 °C measured by Yoko [6] using CV and 6.25×10^{-4} cm^2·s^{-1} at 700 °C by Wang [4] through Warburg coefficient in electrochemical impedance spectroscopy (EIS). The significant difference between our result and that in Ref. [4] may be derived from the different experimental methods. Although Warburg coefficient in EIS can be used to calculate the diffusion coefficient, the calculated value depends strongly on the selected equivalent circuit model and the diffusion species. Unfortunately, it is very difficult to determine the appropriate model as well as the species involved in the diffusion process.

For a soluble-insoluble process, the diffusion coefficient of Cr(II) can be calculated using Delahay equation shown as follows

$$I_{p,2c} = -0.61nFSC_{Cr^{2+}} \left(\frac{nF}{RT}\right)^{0.5} D_{Cr^{2+}}^{0.5} v^{0.5} \tag{3}$$

Assuming that the melt was initially free of Cr^{2+} and $C_{Cr^{2+}} = C_{Cr^{3+}}$ [14], the diffusion coefficient of Cr^{2+} was calculated using the equation

$$I_{p,2c} = -0.61nFSC_{Cr^{3+}} \left(\frac{nF}{RT}\right)^{0.5} D_{Cr^{2+}}^{0.5} v^{0.5} \tag{4}$$

The calculated $D_{Cr^{2+}}$ is $(3.68\pm0.09)\times10^{-6}$ cm^2·s^{-1} at 700 °C. It was noticed that $D_{Cr^{2+}}$ value was slightly larger than $D_{Cr^{3+}}$. The complex ion of chromium like [CrF$_3$]$^{3+}$ may be present in FLiNaK salt, which will reduce the mobility [8, 14].

From the CV curve, the apparent standard potential was calculated from the cathodic peak potentials. For a reversible soluble-insoluble transition, the cathodic peak potential can be expressed as

$$E_{p,2c} = E_{Cr^{2+}/Cr^0}^0 + \frac{RT}{nF}\ln\left(\frac{a_{Cr^{2+}}}{a_{Cr^0}}\right) - 0.854\frac{RT}{nF} \tag{5}$$

or

$$E_{p,2c} = E_{Cr^{2+}/Cr^0}^0 + \frac{RT}{nF}\ln\left(\frac{\gamma_{Cr^{2+}}}{\gamma_{Cr^0}}\right) + \frac{RT}{nF}\ln\left(\frac{X_{Cr^{2+}}}{X_{Cr^0}}\right) - 0.854\frac{RT}{nF} \tag{6}$$

where $E_{p,2c}$ is the cathodic peak potential, E_{Cr^{2+}/Cr^0}^0 is the standard potential, $\gamma_{Cr^{2+}}$ is the activity coefficient ($a_{Cr^{2+}} = \gamma_{Cr^{2+}} X_{Cr^{2+}}$) and $X_{Cr^{2+}}$ is the mole fraction of Cr^{2+} in the FLiNaK. Assuming that the activity of the chromium metal is unity, Eq. (6) can be rewritten to

$$E_{p,2c} = E_{Cr^{2+}/Cr^0}^{0*} + \frac{RT}{nF}\ln\left(X_{Cr^{2+}}\right) - 0.854\frac{RT}{nF} \tag{7}$$

where $E^{0*}_{Cr^{2+}/Cr^0}$ is the apparent standard potential.

For a reversible soluble-soluble transition, the apparent standard potential can be calculated using the following equations proposed by Matsuda and Ayabe [15].

$$E_{1/2} = \left(\frac{E_{p,1a} + E_{p,1c}}{2}\right) = E^0_{Cr^{3+}/Cr^{2+}} + \frac{RT}{nF}\ln\left(\frac{\gamma_{Cr^{3+}}}{\gamma_{Cr^{2+}}}\right) + \frac{RT}{nF}\ln\left(\frac{\sqrt{D_{Cr^{2+}}}}{\sqrt{D_{Cr^{3+}}}}\right) \qquad (8)$$

$$E^{0*}_{Cr^{3+}/Cr^{2+}} = \left(\frac{E_{p,1a} + E_{p,1c}}{2}\right) - \frac{RT}{nF}\ln\left(\frac{\sqrt{D_{Cr^{2+}}}}{\sqrt{D_{Cr^{3+}}}}\right) \qquad (9)$$

where $E_{1/2}$ is the half wave potential. Using Eqs. (7) and (9), the apparent standard potentials of Cr^{2+}/Cr^0 and Cr^{3+}/Cr^{2+} were calculated to be -0.152V (vs. Pt) and -0.215V (vs. Pt), respectively.

3.2. Square wave voltammetry

Square wave voltammetry (SWV) has captured a lot of attention as a voltammetric technique for quantitative study, especially due to its high sensibility [16, 17]. It has been widely applied to determine the number of exchanged electrons and accurately study the reversibility of electrode reaction [10]. In this technique, the working electrode is applied by a potential signal which is a superimposition of a symmetrical square wave and a staircase wave with the same position of the forward pulse of the square wave. The reverse pulse of the square wave occurs half way through the staircase step. The current is measured at the ends of the forward pulse and the reverse pulse during each square wave cycle. According to the measured data, a Gaussian-shape peak can be obtained by plotting the difference between the two measurements at each step versus the potential. Each peak is related to an electrochemical reaction. The half-width of the peak ($W_{1/2}$) is associated with the number of exchange electrons [10]:

$$W_{1/2} = 3.52 \times \frac{RT}{nF} \qquad (10)$$

This equation is deduced for a reversible system. It can also be used for other systems if the peak intensity has a linear relationship with the square root of the frequency [18, 19].

Fig. 5 shows the square wave voltammograms of CrF_3 (0.285 wt%) in molten FLiNaK salt at 700 °C at the frequency ranging from 10 Hz to 30 Hz on a tungsten electrode. Two reduction peaks, 1c and 2c, can be observed at approximately -0.18 V (vs. Pt) and -0.45 V (vs. Pt), respectively, as presented in Fig. 6. Fig. 7 plots the relationship between the peak current density and the square root of the signal frequency. A linear relationship was observed in a 10-30 Hz frequency range, re-verifying the reduction mechanism reversibility. Thus, Eq. (3) is valid in the present system. The values of $W_{1/2}$ were measured to be 0.231 V (vs. Pt) for Peak 1c and 0.146 V (vs. Pt) for Peak 2c, which were employed to calculate the number of exchange electrons through Eq. (3). The calculated results are reported in Table 2. The averages of n_1 and n_2 are 1.28 and 2.02, respectively. This indicates that the electrochemical reduction mechanism of Cr(III) involves two steps: the reductions of Cr(III) to Cr(II) and Cr(II) to Cr. These results are in accordance with those obtained from CV analysis. In addition, it

can be seen from Fig. 5 that Peak 2c is not symmetrical, which is associated with Cr deposition and attributed to the nucleation effect [10].
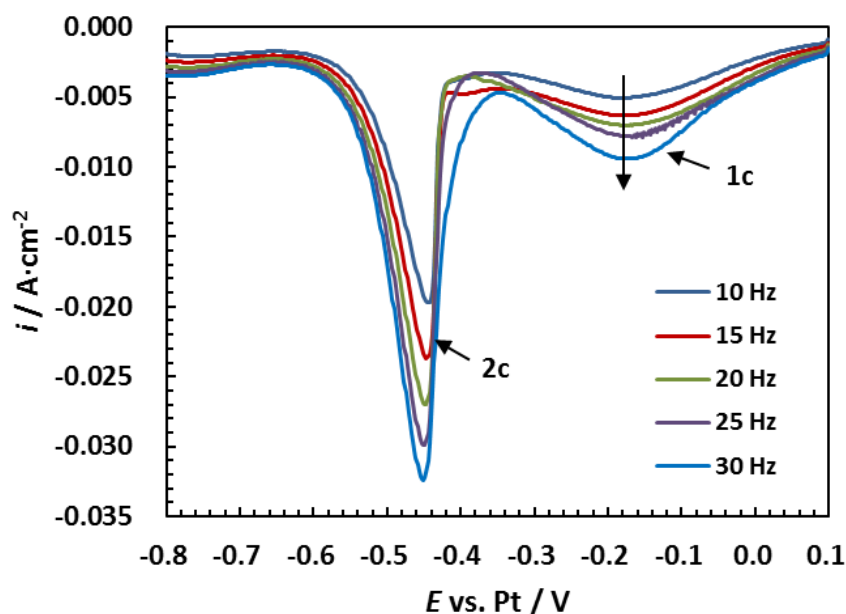

Figure 5. Square wave voltammograms of 0.285 wt% CrF_3 in molten FLiNaK salt at 700 °C, working electrode: W (φ=1.6 mm, surface area: 0.643 cm^2), counter electrode: W (φ=4.0 mm), reference electrode: Pt wire.
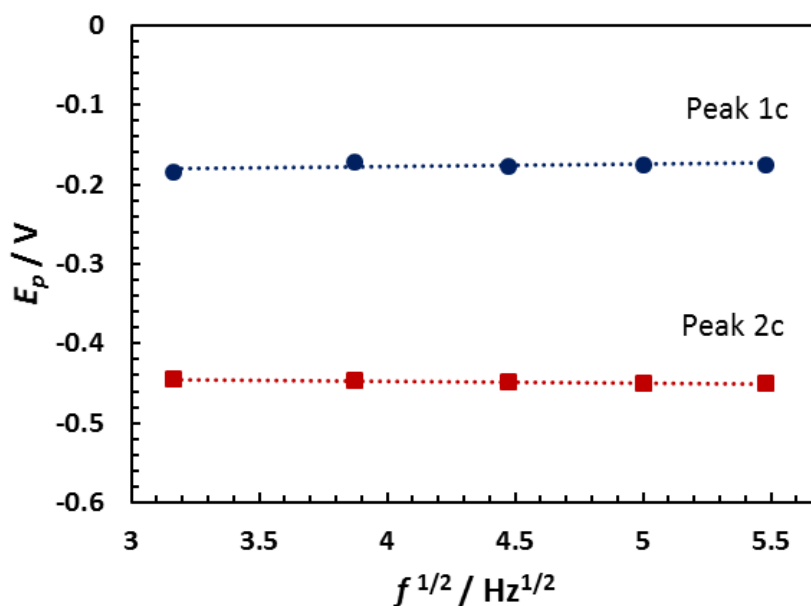

Figure 6. Plot of peak potential versus the square root of the frequency for reduction Peak 1c and Peak 2c in FLiNaK-CrF_3 (0.285 wt%) at 700 °C.
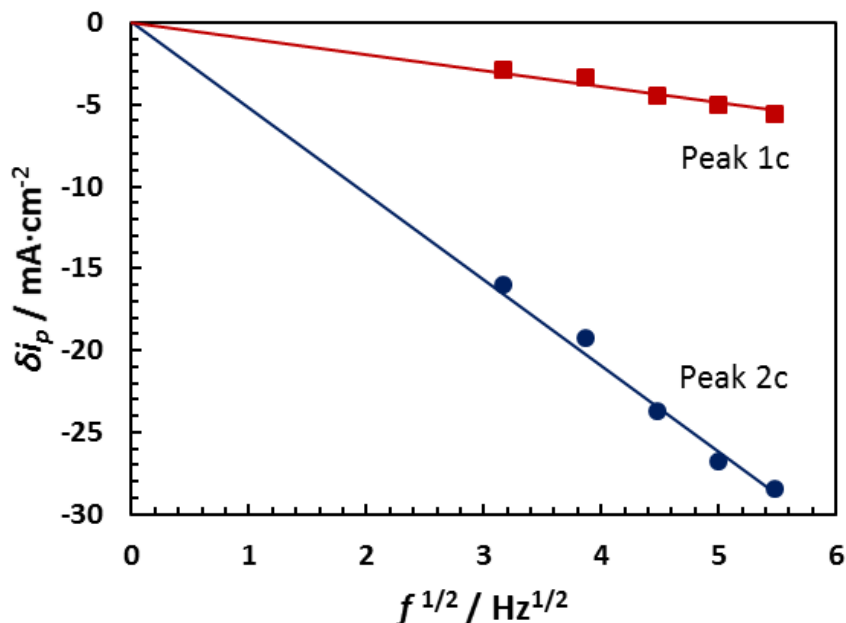
Figure 7. Linear relationship of CrF_3 reduction peak current density versus the square root of the frequency in FLiNaK-CrF_3 (0.285 wt%) at 700 °C.

Table 2. The calculated number of exchanged electrons for Cr(III) reduction process.

f (Hz)	10	15	20	25	30
n_1	1.30	1.33	1.20	1.25	1.32
n_2	1.99	1.91	2.24	2.07	1.92

4. CONCLUSIONS

The electrochemical properties and kinetics of Cr(III) in molten FLiNaK salt at 700 °C were studied through cyclic voltammetry (CV) and square wave voltammetry (SWV). It has been confirmed that Cr(III) was reduced to Cr(0) by a two-step mechanism, vice versa. The reduction of Cr(III) to Cr(II) and Cr(II) to Cr(0) proceed by a single electron and a two-electron exchange, respectively. The kinetic investigation by CV shows the Cr(III)/Cr(II) and Cr(II)/Cr(0) electrochemical systems are limited by the diffusion of electroactive species in melt when the scan rate is below 400 mV/s. The diffusion coefficients of Cr(III) and Cr(II) as well as the apparent potentials of Cr(III)/Cr(II) and Cr(II)/Cr(0) were obtained.

References

1. J. Serp, M. Allibert, O. Beneš, S. Delpech, O. Feynberg, V. Ghetta, D. Heuer, D. Holcomb and V. Ignatiev, *Prog. Nucl. Energ.*, 77 (2014) 308.
2. G.L. Yoder, A. Aaron, B. Cunningham, D. Fugate, D. Holcomb, R. Kisner, F. Peretz, K. Robb, J. Wilgen and D. Wilson, *Ann. Nucl. Energy*, 64 (2014) 511.
3. S. Delpech, C. Cabet, C. Slim and G.S. Picard, *Mater. Today*, 13 (2010) 34.
4. Y.L. Wang, Q. Wang, H.J. Liu and C.L. Zeng, *Corros. Sci.*, 103 (2016) 268.
5. A. Robin and J. De Lépinay, *Electrochim. Acta*, 37 (1992) 2433.
6. T. Yoko and R.A. Bailey, *J. Electrochem. Soc.*, 131 (1984) 2590.
7. D. Ludwig, L. Olson, K. Sridharan, M. Anderson and T. Allen, *Corros. Eng. Sci. Techn.*, 46 (2011) 360.
8. H. Peng, M. Shen, C. Wang, T. Su, Y. Zuo and L. Xie, *RSC Adv.*, 5 (2015) 76689.
9. Y. Berghoute, A. Salmi and F Lantelme, *J. Electroanal. Chem.*, 365 (1994) 171.
10. C. Nourry, L. Massot, P. Chamelot and P. Taxil, *Electrochim. Acta*, 53 (2008) 2650.
11. L. Massot, P. Chamelot, L. Cassayre and P. Taxil, *Electrochim. Acta*, 54 (2009) 6361.
12. A.J. Bard and L.R. Faulkner, *Electrochemical Methods: Principles and Applications, 2nd ed.*, Wiley, (2001) New York.
13. M.S. Sohal, M.A. Ebner, P. Sabharwall and P. Sharpe, *Engineering database of liquid salt thermophysical and thermochemical properties,* Idaho National Laboratory, (2010) Idaho Falls, United State.
14. P. Masset, D. Bottomley, R. Konings, R. Malmbeck, A. Rodrigues and J.P. Glatz, *J. Electrochem. Soc.*, 152 (2005) A1109.
15. H. Matsuda and Y. Ayabe, *Berichte der Bunsengesellschaft für physikalische Chemie*, 59 (1955) 494.
16. F. Garay and M. Lovrić, *J. Electroanal. Chem.*, 518 (2002) 91.
17. L. Ramaley and M.S. Krause, *Anal. Chem.*, 41 (1969) 1362.
18. P. Chamelot, L. Massot, L. Cassayre and P. Taxil, *Electrochim. Acta*, 55 (2010) 4758.
19. P. Chamelot, B. Lafage and P. Taxil, *Electrochim. Acta*, 43 (1998) 607.